RPE | Radiation Physics & Engineering
A Peer-Reviewed Journal
Published by K.N. Toosi University of Technology
http://rpe.kntu.ac.ir
Research Article

Radiation Physics and Engineering 2026; ?(?):?–?

EPICS2023-based evaluation of polyboron as a gamma-ray and fast-neutron shielding material

S. M. Nymul Hasan Anik*, Saad Islam, Ali Mahdi

Department of Nuclear Engineering, Faculty of Engineering and technology, University of Dhaka, Dhaka, Bangladesh

HIGHLIGHTS

- EPICS2023-based photon interaction data were used to assess Polyboron as a radiation shielding material.
- Gamma-ray attenuation parameters of Polyboron were evaluated over a broad energy range.
- Exposure and energy absorption buildup factors were calculated to assess deep-penetration shielding behavior.
- Polyboron showed superior fast neutron removal efficiency compared with ordinary concrete.
- Polyboron offers a lightweight dual-purpose shielding option for gamma-ray and fast-neutron fields.

ABSTRACT

The growing demand for lightweight, high-performance shielding in mixed-field radiation environments exposes the critical limitations of traditional heavy materials like ordinary concrete. This study investigates the dual-shielding efficacy of Polyboron, a composite material, demonstrating its capacity to resolve these practical weight-constraint challenges. Utilizing the MATXCOM code and the EPICS2023 photon data library, we evaluate its fundamental radiological parameters including mass attenuation coefficients, buildup factors, and effective atomic numbers (Z_{eff}) to establish its operational viability. Crucially, this investigation reveals a significant engineering advantage: Polyboron delivers superior fast neutron moderation alongside effective gamma-ray attenuation. Specifically, it provides a 1.8% higher fast neutron removal cross-section (Σ_R of 0.1128 cm^{-1} vs. 0.1108 cm^{-1}) and an approximate 9.2% improvement in mass-specific gamma-ray attenuation (MAC) at 1 MeV compared to ordinary concrete. Remarkably, it achieves this enhanced dual-field shielding while offering a massive 57.8% reduction in physical weight (0.971 g.cm^{-3} versus 2.30 g.cm^{-3}). By matching or exceeding these mass-based protective capabilities of conventional concrete at a fraction of the weight, Polyboron is established as a highly efficient, deployment-ready alternative for weight-sensitive nuclear applications.

KEYWORDS
Polyboron
Mass attenuation coefficient
Buildup factor
Neutron removal cross-section
MATXCOM
Phy-X/PSD

HISTORY
Received:
Revised:
Accepted:
Published:

1 Introduction

Radiation shielding is a critical component of safety infrastructure in nuclear power plants, medical facilities, and high-energy physics laboratories. As the demand for versatile and cost-effective shielding grows, locally developed composite materials like Polyboron have emerged as promising candidates due to their favorable physicochemical properties. The effectiveness of such composites relies on their ability to attenuate mixed radiation fields, specifically gamma rays and neutrons, which requires a synergistic composition of high-density elements for photon attenuation and hydrogenous materials for neutron moderation. Polyboron utilizes this principle, combining polyethylene and paraffin wax for neutron moderation with boron ester for thermal neutron capture, resulting in a density of 0.971 g.cm^{-3} (Bhuiyan et al., 1989; Ahmed et al., 1992). Beyond its favorable weight and radiological properties, this high paraffin wax and polyethylene content renders Polyboron highly thermoplastic. While structurally rigid at room temperature, it can be easily melted and cast into complex, custom geometries at relatively low temperatures during fabrication. This excellent moldability provides a distinct operational deployment advantage over traditional concrete or metallic shields, which require bulky formwork, long curing times, or high-temperature smelting.

While the physical fabrication of Polyboron has been

*Corresponding author: smnymulhasananik@gmail.com

https://doi.org/

established, its radiological characterization remains fragmented. In a preliminary investigation, Biswas et al. (Biswas et al., 2016) calculated the mass attenuation coefficient (MAC), linear attenuation coefficient (LAC), and half-value layer (HVL) for Polyboron. However, that study relied on the WinXCOM code, which utilizes older cross-section databases that have since been superseded by more accurate evaluations. Furthermore, the work of Biswas et al. (Biswas et al., 2016) was limited strictly to primary photon attenuation coefficients. It did not account for the complex scattering effects inherent in thick shields, which are quantified by the Exposure Buildup Factor (EBF) and Energy Absorption Buildup Factor (EABF). Additionally, despite Polyborons design intent as a neutron shield, the previous study failed to report the Fast Neutron Removal Cross-section (Σ_R). Relying solely on linear attenuation coefficients without considering buildup factors or neutron interactions can lead to significant underestimations of dose rates in practical shielding designs.

The critical bottleneck in deploying locally developed composites like Polyboron for weight-sensitive nuclear applications is the absence of rigorous, modern qualification of their performance in complex mixed-field environments. To address this engineering gap, this study transitions Polyboron from experimental material synthesis to a deployment-ready shielding alternative by comprehensively evaluating its operational safety parameters. Utilizing the advanced MATXCOM program based on the EPICS2023 evaluated photon data library (Islam, 2025), we establish the precision required for modern shielding engineering. We evaluate critical deployment parameters over a wide energy range (1 keV to 20 MeV), including the Effective Atomic Number (Z_{eff}), Effective Electron Density (N_{eff}), and deep penetration scattering effects quantified by exposure and energy-absorption buildup factors (EBF and EABF). Crucially, we validate the practical advantage of Polyboron by calculating its Fast Neutron Removal Cross-section (Σ_R) and benchmarking it directly against traditional, heavy shielding materials such as ordinary concrete and lead (Ahmed et al., 1992; Biswas et al., 2016). By demonstrating that Polyboron delivers superior dual-field attenuation at a fraction of the structural weight, this work provides the essential engineering justification required for its integration into next-generation, weight-restricted nuclear facilities.

2 Theoretical Background

When ionizing photons (X-rays or gamma rays) traverse a material, they interact via several processes: photoelectric absorption, coherent (Rayleigh) scattering, incoherent (Compton) scattering, and (at higher energies) pair production in nuclear and electron fields. For photon energies below 0.3 MeV, photoelectric absorption (which strongly depends on the atomic number Z) typically dominates. In the intermediate energy range (roughly 0.3-5 MeV), Compton scattering is the primary interaction mechanism, while at energies above 56 MeV, pair production becomes significant (Chilton et al., 1983).

The cumulative probability of all interaction processes per unit path length in a material is described by the linear attenuation coefficient (LAC, μ). The attenuation of a narrow beam of photons, as well as the parameters derived from it, including the mass attenuation coefficient (MAC, μ_m), half-value layer (HVL), and tenth-value layer (TVL) are well-established in radiation shielding physics. For composite materials like Polyboron, the MAC is determined using the standard mixture rule based on the weight fractions of constituent elements. HVL and TVL, which denote the thickness required to attenuate radiation to one-half and one-tenth of its original intensity, respectively, are calculated directly from the LAC based on the Beer-Lambert exponential attenuation law. Because these mathematical formulations are standard, they are not explicitly reproduced here but are described comprehensively in foundational literature (Chilton et al., 1983). Both HVL and TVL provide a practical way to compare the shielding effectiveness of different materials, where lower values indicate more effective shielding.

The Mean Free Path (MFP) is a critical parameter describing the average distance a photon can travel in a material before undergoing an interaction such as absorption or scattering. Mathematically, the MFP is derived from the integral of the exponential attenuation law and is calculated as

$$MFP = \frac{\int_0^\infty t\,\mathrm{e}^{-\mu t}\,\mathrm{d}t}{\int_0^\infty \mathrm{e}^{-\mu t}\,\mathrm{d}t} = \frac{1}{\mu} \tag{1}$$

It is inversely related to the LAC and sometimes referred to as the relaxation length.

The total atomic cross-section (ACS) symbolized as σ_a, represents the effective area that an atom presents for interaction with gamma photons. It is calculated as (Akman et al., 2015):

$$\sigma_a = \frac{\mu_m \sum_i n_i A_i}{N_A \sum_i n_i} \tag{2}$$

where n_i is the number of atoms and A_i is the atomic weight of the i-th constituent element. N_A is Avogadro's constant. The total electronic cross-section (ECS) symbolized as σ_e, provides the effective area that electrons in the material present for interaction with gamma photons. It is calculated as (Han and Demir, 2009a):

$$\sigma_e = \frac{1}{N_A} \sum_i \left(\frac{x_i A_i}{Z_i} \mu_{m,i} \right) \tag{3}$$

where, x_i is the mol fraction, Z_i is the atomic number of the i-th element.

The effective atomic number Z_{eff} is a single-number representation of a compound's overall atomic number in terms of interaction probabilities. Z_{eff} is defined such that the compounds attenuation for a given process (e.g., Compton scattering, photoelectric effect) is equivalent to that of a hypothetical element with atomic number Z_{eff}.

The effective atomic number can be determined using the relationship between σ_a and σ_e:

$$Z_{eff} = \frac{\sigma_a}{\sigma_e} \tag{4}$$

The effective electron density (N_{eff}) is a parameter that represents the number of electrons per unit mass in a material. A higher N_{eff} value means that there are more electrons available per unit mass for interaction, leading to higher probabilities of scattering and absorption events. The N_{eff} can be derived using MAC and the σ_e (Han and Demir, 2009b):

$$N_{eff} = \frac{\mu_m}{\sigma_e} \tag{5}$$

Effective Conductivity (C_{eff}) is a parameter that quantifies the electrical conductivity of a material, considering its N_{eff}. It is a significant property in materials science, particularly in the study of conductive materials and their interactions with electromagnetic fields. The C_{eff} of a material is directly proportional to its N_{eff} and is given by the following equation (Manjunatha, 2017)

$$C_{eff} = \frac{N_{eff}\,\rho e^2 \tau}{m_e} \tag{6}$$

where, e is the elementary charge, τ is the average lifetime (relaxation time) of an electron at the Fermi surface, and m_e is the mass of an electron.

When gamma photons penetrate a material, they undergo interactions such as scattering and absorption. These interactions result in the buildup of secondary radiation within the material. To accurately assess the radiation exposure and energy deposition, it is essential to consider the buildup factors, namely the Exposure Buildup Factor (EBF) and the Energy Absorption Buildup Factor (EABF). Mathematically, the EBF and the EABF modify the Beer-Lambert law as

$$I = BI_0 e^{-\mu t} \tag{7}$$

where B is the buildup factor.

EBF is defined as the ratio of the total exposure at a point, considering both primary and scattered photons, to the exposure from only primary photons. An EBF greater than 1 indicates that scattered photons contribute to the dose at that point. Similarly, EABF is defined as the ratio of the total energy absorbed in the material (including contributions from secondary interactions) to the energy absorbed from the primary photons alone. EABF is useful for estimating the overall energy deposition within the material.

The calculation procedures for EBF and EABF are similar, differing mainly in the coefficients used from standard databases, and often employs the Geometric Progression (G-P) fitting method. The G-P fitting method involves several steps described as follows. First, the ratio of Compton to total MAC is calculated

$$R = \frac{(\mu_m)_{\text{Compton}}}{(\mu_m)_{\text{Total}}} \tag{8}$$

The R value must be between the corresponding values for two adjacent elements. Using R, the so called Equivalent Atomic Number (Z_{eq}) is calculated:

$$Z_{eq} = \frac{Z_1(\log R_2 - \log R) + Z_2(\log R - \log R_1)}{\log R_2 - \log R_1} \tag{9}$$

where R_1 and R_2 are the $(\mu_m)_{\text{Compton}}/\mu_m$ ratios for elements with atomic numbers Z_1 and Z_2, respectively. Using Z_{eq}, the G-P fitting parameters a, b, c, d, and X_K are interpolated (Harima, 1983) from tabulated values (Trubey et al., 1991).

$$P = \frac{P_1(\log Z_2 - \log Z_{eq}) + P_2(\log Z_{eq} - \log Z_1)}{\log Z_2 - \log Z_1} \tag{10}$$

where P represents any of the G-P fitting parameters.

The buildup factor $B(E, X)$ is calculated using:

$$B(E,X) = \begin{cases} 1 + \dfrac{(b-1)(K^X - 1)}{K - 1} & \text{for } K \neq 1 \\ 1 + (b-1)X & \text{for } K = 1 \end{cases} \tag{11}$$

where $K(E, X)$ is given by:

$$K(E,X) = CX^a + d\frac{\tanh\left(\dfrac{X}{X^K} - 2\right) - \tanh(-2)}{1 - \tanh(-2)} \tag{12}$$

Z_{eq} values and the GP fitting parameters of polyboron, calculated by MATXCOM, are given in Table 1.

Table 1: Polyboron GP fitting parameters for EBF in the range of 0.015-15 MeV.

Energy (MeV)	Z_{eq}	a	b	c	d	X_K
0.015	6.08	0.15	1.37	0.53	-0.07	14.31
0.02	6.09	0.08	1.85	0.72	-0.04	16.42
0.03	6.07	-0.02	3.44	1.13	0.01	13.04
0.04	6.04	-0.13	5.2	1.72	0.06	13.9
0.05	6.01	-0.17	6.69	2.1	0.07	14.34
0.06	5.97	-0.2	7.24	2.4	0.09	14.53
0.08	5.91	-0.23	6.88	2.73	0.1	14.46
0.1	5.86	-0.24	6.19	2.84	0.1	14.61
0.15	5.79	-0.25	4.68	2.91	0.11	14.38
0.2	5.75	-0.24	3.79	2.82	0.11	14.86
0.3	5.71	-0.23	3.15	2.55	0.1	14.29
0.4	5.69	-0.21	2.85	2.32	0.09	13.21
0.5	5.7	-0.19	2.66	2.11	0.09	13.76
0.6	5.68	-0.17	2.54	1.94	0.07	13.63
0.8	5.67	-0.14	2.33	1.75	0.07	13.67
1	5.68	-0.12	2.21	1.58	0.06	13.7
1.5	5.38	-0.08	2.05	1.35	0.04	13.74
2	5.3	-0.05	1.94	1.21	0.03	14.3
3	5.28	-0.02	1.78	1.07	0.01	12.52
4	5.27	0.01	1.68	0.98	-0.01	19.59
5	5.27	0.02	1.59	0.93	-0.01	14.82
6	5.27	0.03	1.54	0.91	-0.01	14.76
8	5.27	0.04	1.45	0.87	-0.02	14.99
10	5.27	0.04	1.38	0.85	-0.02	13.12
15	5.26	0.05	1.28	0.83	-0.03	14.36

Table 2: Polyboron GP fitting parameters for EABF in the range of 0.015-15 MeV.

Energy (MeV)	Z_{eq}	a	b	c	d	X_K
0.015	6.08	0.15	1.38	0.52	-0.08	14.43
0.02	6.09	0.08	1.87	0.72	-0.04	16.31
0.03	6.07	-0.02	3.65	1.13	0.01	12.83
0.04	6.04	-0.12	5.02	1.71	0.05	14.09
0.05	6.01	-0.16	5.59	2.06	0.07	14.47
0.06	5.97	-0.19	5.42	2.3	0.08	14.66
0.08	5.91	-0.21	4.84	2.51	0.08	14.83
0.1	5.86	-0.21	4.27	2.58	0.08	14.94
0.15	5.79	-0.2	3.55	2.48	0.07	15.39
0.2	5.75	-0.19	3.19	2.36	0.07	15.5
0.3	5.71	-0.18	2.78	2.15	0.07	15.01
0.4	5.69	-0.16	2.6	1.95	0.06	14.7
0.5	5.7	-0.14	2.45	1.82	0.06	15.62
0.6	5.68	-0.12	2.39	1.68	0.05	14.9
0.8	5.67	-0.11	2.19	1.57	0.05	14.11
1	5.68	-0.09	2.09	1.47	0.04	14.13
1.5	5.38	-0.06	1.94	1.28	0.03	14.33
2	5.3	-0.04	1.84	1.18	0.02	14.26
3	5.28	-0.01	1.72	1.05	0	13.39
4	5.27	0	1.63	0.99	0	14.34
5	5.27	0.02	1.57	0.94	-0.01	14.18
6	5.27	0.03	1.52	0.9	-0.02	12.93
8	5.27	0.04	1.45	0.86	-0.02	11.42
10	5.27	0.04	1.39	0.86	-0.02	14.46
15	5.26	0.05	1.29	0.84	-0.03	14.57

Finally, for neutron shielding capability, the key parameter is the fast neutron removal cross-section Σ_R (usually in units of cm^{-1}). Σ_R represents an approximate measure of the probability per unit path length that a fast neutron will be removed from a beam via all possible interactions (primarily scatter or absorption leading to thermalization or capture) in the material. It is not a sharply defined cross-section for a single reaction, but an aggregate measure useful for comparing materials' effectiveness against fast neutrons. With the introduction of Σ_R, the attenuation of fast neutrons in matter follows an exponential law similar to that for gamma rays

$$\varphi = \varphi_0 \mathrm{e}^{-\Sigma_R x} \tag{13}$$

where φ_0 and φ are the initial and the transmitted neutron flux, respectively. For homogeneous mixtures, the effective fast neutron removal cross-section can be expressed as

$$\Sigma_R = \sum_i w_i \left(\frac{\Sigma_R}{\rho}\right)_i \tag{14}$$

where w_i is the weight percentage, and $(\frac{\Sigma_R}{\rho})_i$ is the mass removal cross-section of the i-th constituent. Empirical models are often used to estimate Σ_R/ρ for elements without experimentally measured values. Zoller proposes one such model (Zoller, 1964) which gives an approximate value of the fast neutron mass removal cross-section:

$$\frac{\Sigma_R}{\rho} = \begin{cases} 0.190\, Z^{-0.743} & \text{for } Z \leq 8 \\ 0.125\, Z^{-0.565} & \text{for } Z > 8 \end{cases} \tag{15}$$

where Z is the atomic number. The fast neutron removal cross-section is essential for evaluating the neutron shielding capabilities of materials. Higher values of Σ_R indicate better neutron attenuation properties, making such materials preferable for applications in nuclear reactors, radiation protection, and other environments where neutron flux must be minimized.

3 Materials and Methods

In the present work, attenuation parameters for polyboron and a set of reference shielding materials (ordinary concrete, lead, borated polyethylene, non-borated polyethylene, and water) were computed using MATXCOM and PhyX-PSD. MATXCOM is a specialized program developed for calculating x-ray and gamma-ray interaction cross-sections and attenuation parameters for arbitrary material compositions (Islam, 2025). It is based on the EPICS2023 evaluated photon data library (EPDL), which is part of the forthcoming ENDF/B-VIII.1 nuclear data release, ensuring that the most current interaction data are employed. MATXCOM computes the total and partial interaction cross-sections (covering photoelectric absorption, coherent and incoherent scattering, and pair production) over an energy range from 1 keV to 100 GeV. From these data, it derives the mass attenuation coefficient (MAC) and, by extension, the linear attenuation coefficient (LAC), mean free path (MFP), half-value layer (HVL), and tenth-value layer (TVL) using established relationships. In addition, MATXCOM determines the effective atomic number (Z_{eff}), effective electron density (N_{eff}), effective conductivity (C_{eff}), and the total atomic (σ_a) and electronic cross-sections (σ_e) based on standard mixture rules. The program also calculates the exposure buildup factor (EBF) and energy-absorption buildup factor (EABF) through the Geometric Progression (G-P) fitting method, which interpolates standard fitting parameters over a defined energy grid and various penetration depths. It is important to note that because MATXCOM and Phy-X/PSD function as analytical computational tools rather than stochastic Monte Carlo transport solvers, they do not require explicit user definitions for source geometry, dimensions, or angular distribution. Fundamental parameters such as the MAC, LAC, and Z_{eff} are intrinsic material properties that depend strictly on the elemental composition and incident photon energy. For the calculated EBF and EABF, the standard databases underlying the G-P fitting method inherently assume a theoretical point isotropic source within an infinite homogeneous medium. This idealized geometry removes geometry-dependent scattering artifacts, providing a universal and standardized benchmark for comparing the intrinsic shielding efficacies of different materials.

PhyX-PSD is a well-established online software for calculating radiation shielding and dosimetry parameters (Şakar et al., 2020). It implements algorithms to compute attenuation coefficients, buildup factors, and the fast neutron removal cross-section (Σ_R). In our study, PhyX-PSD is used as a benchmark for validating the MATXCOM results. For Σ_R, additional calculations were made based on

Table 3: Elemental composition of different shielding materials. Polyboron: Density (g.cm^{-3}) = 0.971, Total atom density (atoms/b-cm) = 1.120 E-01. Concrete, Ordinary Density (g.cm^{-3}) = 2.300000 Total atom density (atoms/b-cm) = 9.946E-02. Polyethylene, Borated: Density (g.cm^{-3}) = 1.000000, Total atom density (atoms/b-cm) = 1.193E-01. Polyethylene, Non-borated: Density (g.cm^{-3}) = 0.930000, Total atom density (atoms/b-cm) = 1.198E-01. Water: Density (g.cm^{-3}) = 0.998207, Total atom density (atoms/b-cm) = 1.001E-01.

	Polyboron		Concrete, Ordinary		Polyethylene, Borated		Polyethylene, Non-borated		Water	
Element	Weight Fraction	Atom Fraction	Weight Fraction	Atom Fraction	Weight Fraction	Atom Fraction	Weight Fraction	Atom Fraction	Weight Fraction	Atom Fraction
H	0.123800	0.641432	0.022100	0.305330	0.125355	0.627759	0.143716	0.666662	0.111894	0.666657
B	0.048900	0.023622	-	-	0.100000	0.046690	-	-	-	-
C	0.598800	0.260362	0.002484	0.002880	0.774645	0.325552	0.856284	0.333338	-	-
O	0.228500	0.074584	0.574930	0.500407	-	-	-	-	0.888106	0.333343
Na	-	-	0.015208	0.009212	-	-	-	-	-	-
- Mg	-	-	0.001266	0.000725	-	-	-	-	-	-
Al	-	-	0.019953	0.010298	-	-	-	-	-	-
Si	-	-	0.304627	0.151042	-	-	-	-	-	-
S	-	-	-	-	-	-	-	-	-	-
K	-	-	0.010045	0.003578	-	-	-	-	-	-
Ca	-	-	0.042951	0.014924	-	-	-	-	-	-
Fe	-	-	0.006435	0.001605	-	-	-	-	-	-

the fast neutron mass removal cross-sections reported by Hila et al. (Hila et al., 2023) and correlations proposed by Zollar (Zoller, 1964) for comparison with the PhyX-PSD values.

The modeling of Polyboron in this study is strictly grounded in the experimentally established formulation described by Ahmed et al. (Ahmed et al., 1992), ensuring that the simulated material represents a physically realizable and mechanically proven composite. The elemental composition is derived from the standard weight ratio of polyethylene, boron ester, and paraffin wax (16.5:37.5:46) used in the physical fabrication of the material. By applying the high-precision EPICS2023 data library to this specific, standardized composition, this work aims to establish a definitive reference database for the material. Providing these pre-calculated, validated parameters allows nuclear engineers and shield designers to accurately integrate Polyboron into safety systems without the need to repeat computationally expensive and time-consuming Monte Carlo simulations for routine radiological assessments. The details for ordinary concrete (NIST), borated polyethylene, and non-borated polyethylene were taken from Detwiler et al. (Detwiler et al., 2021). The elemental compositions of these shielding materials are provided in Table 3.

Polyboron density is estimated to be accurate to 3 significant digits. Uncertainties are not addressed. Concrete, borated and non-borated polyethylenes, and water have estimated accuracies of 2, 3, 2, and 5 significant digits, respectively.

4 Results and Discussion

4.1 Gamma-Ray Attenuation Parameters

MAC and LAC are pivotal in understanding the shielding capabilities of materials. MAC represents the probability of interaction per unit mass, while LAC indicates the probability of interaction per unit length. Together, these coefficients offer a comprehensive picture of how effectively a material can attenuate radiation. The MAC and LAC values for polyboron, compared to ordinary concrete, borated polyethylene, non-borated polyethylene, and water, are shown in Figs. 3 and 4.

For polyboron, the MAC values are high at lower energies, such as 2432.604 cm^2.g^{-1} at 0.001 MeV, showing strong attenuation properties. Compared to materials like ordinary concrete (3464.644 cm^2.g^{-1}), borated polyethylene (1835.268 cm^2.g^{-1}), non-borated polyethylene (1894.020 cm^2.g^{-1}), and water (4076.151 cm^2.g^{-1}), polyboron is competitive, though concrete and water are slightly higher at this energy. As photon energy increases, MAC values decrease; at 1 MeV, polyboron's MAC is 0.071 cm^2.g^{-1}, slightly higher than concrete's 0.065 cm^2.g^{-1}, indicating its effectiveness across various energies. MAC values computed by MATXCOM were found to be in excellent agreement with those computed by Phy-X/PSD. This comparison is visually demonstrated in Fig. 1 across the continuous incident photon energy spectrum, and in Fig. 2 for common discrete gamma-ray source energies.

The LAC for polyboron at 0.001 MeV is 2362.059 cm^{-1}, lower than concrete's 7968.681 cm^{-1}, but still significant. At 1 MeV, polyboron's LAC is 0.069 cm^{-1}, whereas for concrete it is 0.149 cm^{-1}.

The HVL and TVL values for polyboron, compared to ordinary concrete, borated polyethylene, non-borated polyethylene, and water, are shown in Figs. 5 and 6. At very low photon energies, polyboron exhibits lower HVL and TVL values. However, as the energy increases to 0.1 MeV, polyboron requires a greater physical thickness (HVL of 4.217 cm and TVL of 14.008 cm) to attenuate radiation compared to the much denser ordinary concrete (1.733 cm and 5.758 cm, respectively). This behavior confirms that heavy concrete provides superior volume-based gamma shielding.

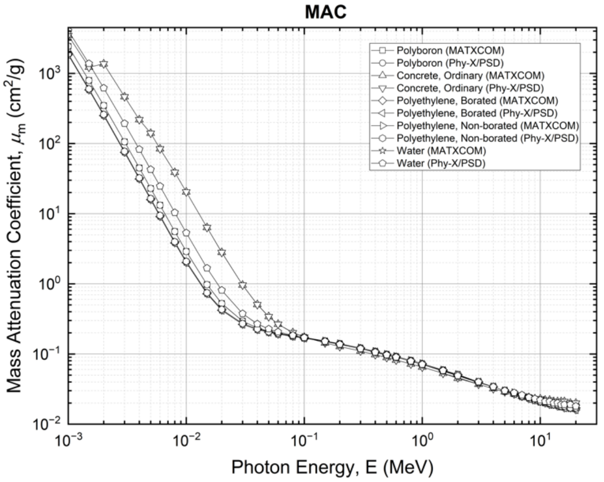

Figure 1: Comparison of the mass attenuation coefficients (MAC) computed by MATXCOM and Phy-X/PSD as a function of incident photon energy for Polyboron and reference shielding materials.

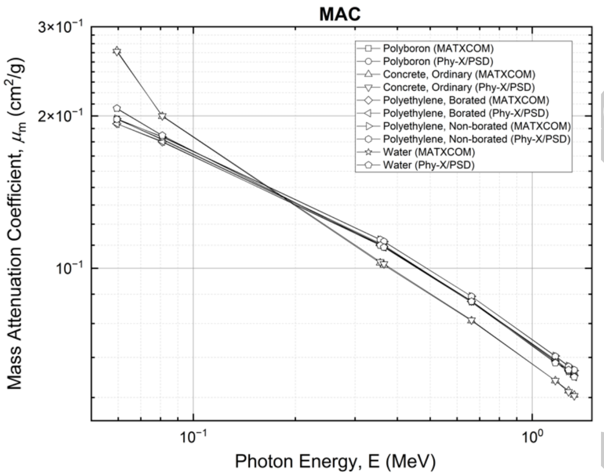

Figure 2: Comparison of the mass attenuation coefficients (MAC) computed by MATXCOM and Phy-X/PSD for Polyboron and reference shielding materials at common discrete gamma-ray source energies.

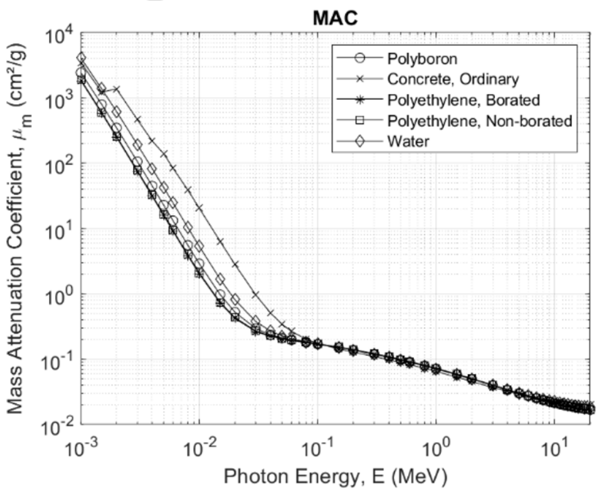

Figure 3: MAC of shielding materials as a function of incident photon energy.

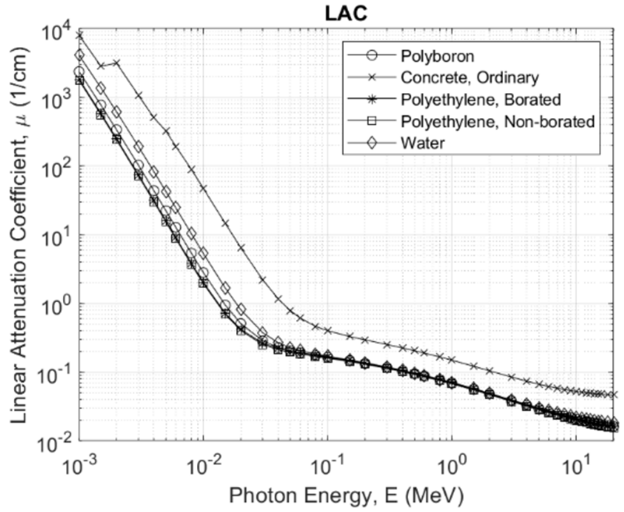

Figure 4: LAC of shielding materials as a function of incident photon energy.

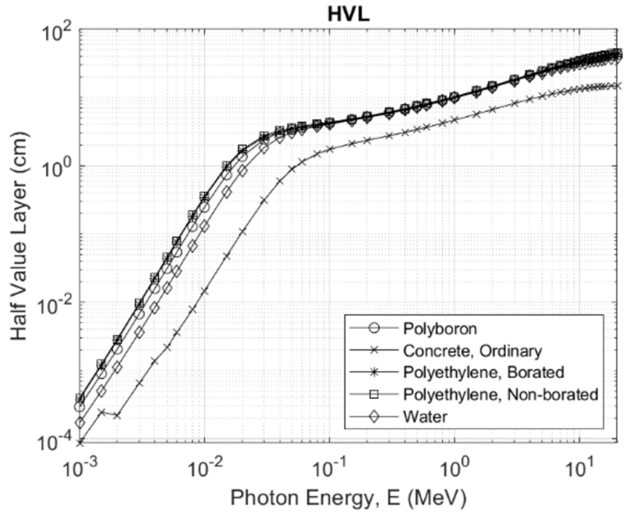

Figure 5: HVL of shielding materials as a function of incident photon energy.

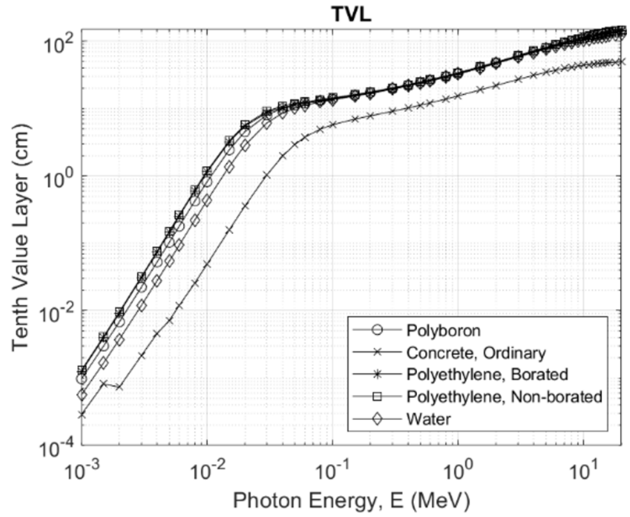

Figure 6: TVL of shielding materials as a function of incident photon energy.

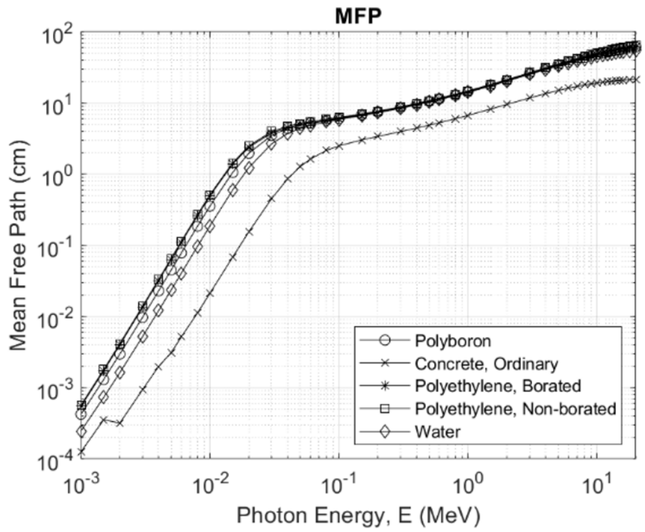

Figure 7: MFP of shielding materials as a function of incident photon energy.

However, evaluating shields solely based on absolute thickness (cm) obscures the primary deployment advantage of Polyboron: its structural weight. To quantitatively compare the weight of the two shields, we calculate the required mass thickness (areal density, g.cm^{-2}) needed to achieve a specific level of attenuation. Mass thickness is mathematically derived as the physical thickness multiplied by the material density ($\rho\times$TVL), which is inversely proportional to the MAC. At an intermediate photon energy of 1 MeV, concrete requires an areal density of 35.42 g.cm^{-2} to achieve a ten-fold reduction in gamma intensity (1 TVL). In contrast, due to its higher MAC at this energy, Polyboron achieves the exact same 10-fold gamma reduction with an areal density of only 32.43 g.cm^{-2}. Consequently, despite requiring a physically thicker barrier, a Polyboron shield is approximately 8.4% lighter than an ordinary concrete shield for equivalent gamma attenuation at 1 MeV. This quantitative weight reduction establishes its superiority for weight-restricted applications.

At 0.001 MeV, the MFP for polyboron is significantly lower than that of other materials, as shown in Fig. 7, indicating a higher probability of photon interactions within a shorter distance. Even at higher energies, such as 1 MeV, polyboron shows an MFP of 14.487 cm, which is comparable to ordinary concrete but better than borated and non-borated polyethylene. These values are significant because they illustrate that polyboron requires less or comparable thickness to achieve the same level of radiation protection compared to shielding materials like concrete and polyethylene.

N_{eff} reflects the number of electrons per unit mass that can participate in photon attenuation processes. In comparing polyboron to other shielding materials such as ordinary concrete, borated polyethylene, non-borated polyethylene, and water, polyboron as shown in Fig. 8 shows a higher N_{eff} across various photon energies. At lower energies, polyboron exhibits an N_{eff} of 7.70×10^{23} e.g^{-1} at 0.001 MeV, which is significantly higher than concrete (3.92×10^{23} e.g^{-1}) and similar to that of water (8.01×10^{23} e.g^{-1}).

In the comparison of polyboron with ordinary concrete, borated polyethylene, non-borated polyethylene, and water, as shown in Fig. 9, polyboron exhibits a consistently high C_{eff}, particularly at lower photon energies. For instance, at 0.001 MeV, polyboron has an effective conductivity of 5.36×10^{8} S.m^{-1}, which is lower than concrete (6.46×10^{8} S.m^{-1}) but higher than both types of polyethylene and water. As the photon energy increases, polyboron's C_{eff} remains stable and competitive. Materials with higher conductivity are generally better at absorbing and dissipating electromagnetic energy. At higher photon energies, the conductivity values of all materials converge.

The variation in ACS with respect to incident photon energy is shown in Fig. 10. Across the incident photon energies, polyboron demonstrates a relatively lower ACS compared to ordinary concrete but higher than that of borated and non-borated polyethylene and water, particularly at lower photon energies. For instance, at 0.001 MeV, polyboron has an ACS of 2.11×10^{4} b, which is lower than concrete (8.01×10^{4} b) but higher than borated polyethylene (1.54×10^{4} b). At 1 MeV, polyboron's ACS stabilizes around 0.594 b, slightly higher than polyethylene-based materials but lower than concrete, signifying its balanced shielding capability.

The variation in ECS with respect to incident photon energy is shown in Fig. 11. ECS indicates the probability of photon interactions with electrons in the material, which is crucial for understanding how effectively the material can attenuate radiation. Across various photon energies, polyboron demonstrates a moderate ECS, typically higher than polyethylene-based materials but lower than ordinary concrete. For instance, at 0.001 MeV, polyboron's ECS is 3.16×10^{3} b, lower than concrete (8.85×10^{3} b) but higher than borated polyethylene (2.60×10^{3} b). As photon energy increases, polyboron's σ_e decreases, indicating a reduced probability of electron interaction at higher energies. At 1 MeV, polyboron's ECS is 0.211 b, comparable to borated polyethylene and water but lower than concrete.

Polyboron consistently shows a lower Z_{eff} compared to ordinary concrete across the entire energy range from 0.001 MeV to 20 MeV, as shown in Fig. 12, indicating its lower density and atomic number. This characteristic suggests that polyboron may not attenuate medium to high-energy photons as effectively as concrete, which has a higher Z_{eff} and thus greater photon interaction probabilities. However, polyboron performs comparably or better than borated and non-borated polyethylene and water, which exhibit similar or slightly lower Z_{eff} values. At lower photon energies, polyboron's Z_{eff} remains stable around 6.7, indicating its consistent performance in attenuating low-energy photons, albeit less effectively than materials with higher atomic numbers like concrete. This makes polyboron suitable for applications requiring photon attenuation at a moderate to low level of energy.

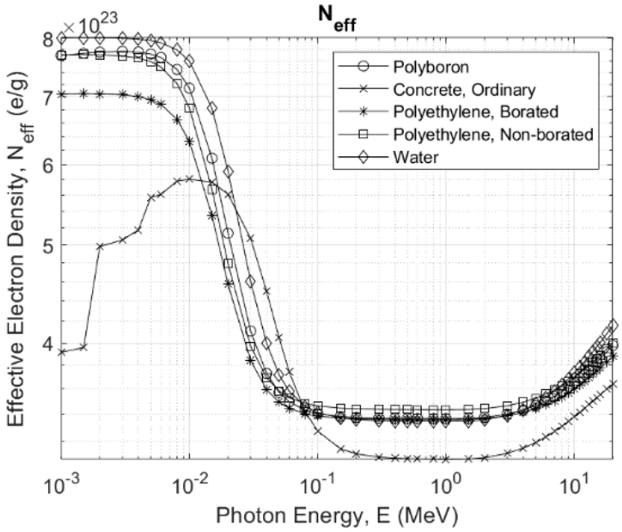

Figure 8: eff of shielding materials as a function of incident photon energy.

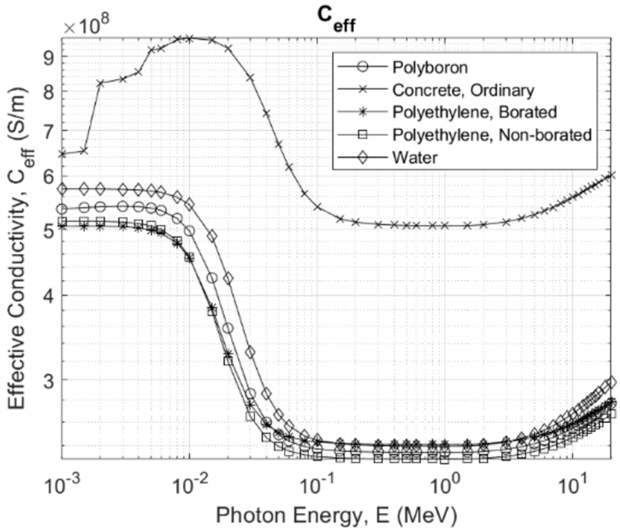

Figure 9: eff of shielding materials as a function of incident photon energy.

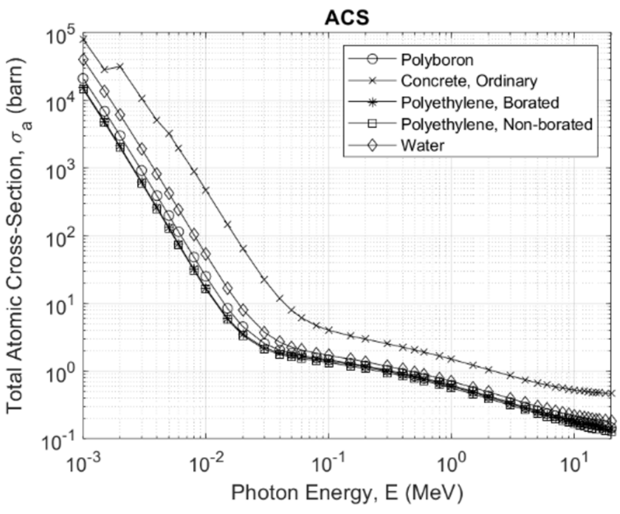

Figure 10: a of shielding materials as a function of incident photon energy.

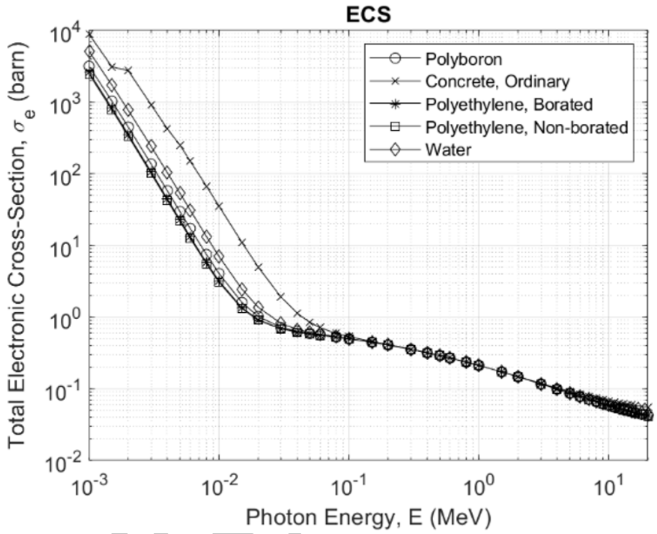

Figure 11: e of shielding materials as a function of incident photon energy.

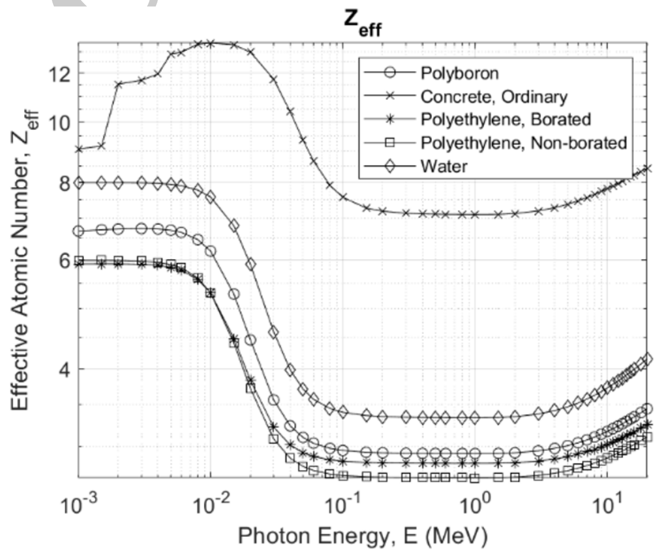

Figure 12: eff of shielding materials as a function of incident photon energy.

The variation in the EBF with photon energy at fixed penetration depths of 1, 5, 10, and 40 MFP are shown in Fig. 13-a to 13-d. The EBF values for shielding materials ranged between photon incident energy of 0.015 and 10 MeV. It is apparent from the figures that the EBF increases with incident photon energy, reaching a peak before decreasing as photon energy continues to increase. This peak corresponds to the dominance of Compton scattering interactions. At medium energies, particularly between 0.08 and 0.2 MeV, the EBF values are significantly high at penetration depths of 10 and 40 MFP. In this energy range, γ-ray photons undergo multiple Compton scattering events, reducing their energies but not entirely removing them from the material, thus elevating the EBF. However, as photon energy continues to rise, pair production becomes more significant, diminishing the impact of Compton scattering. This shift leads to a gradual decrease in EBF values at higher photon energies. At 1

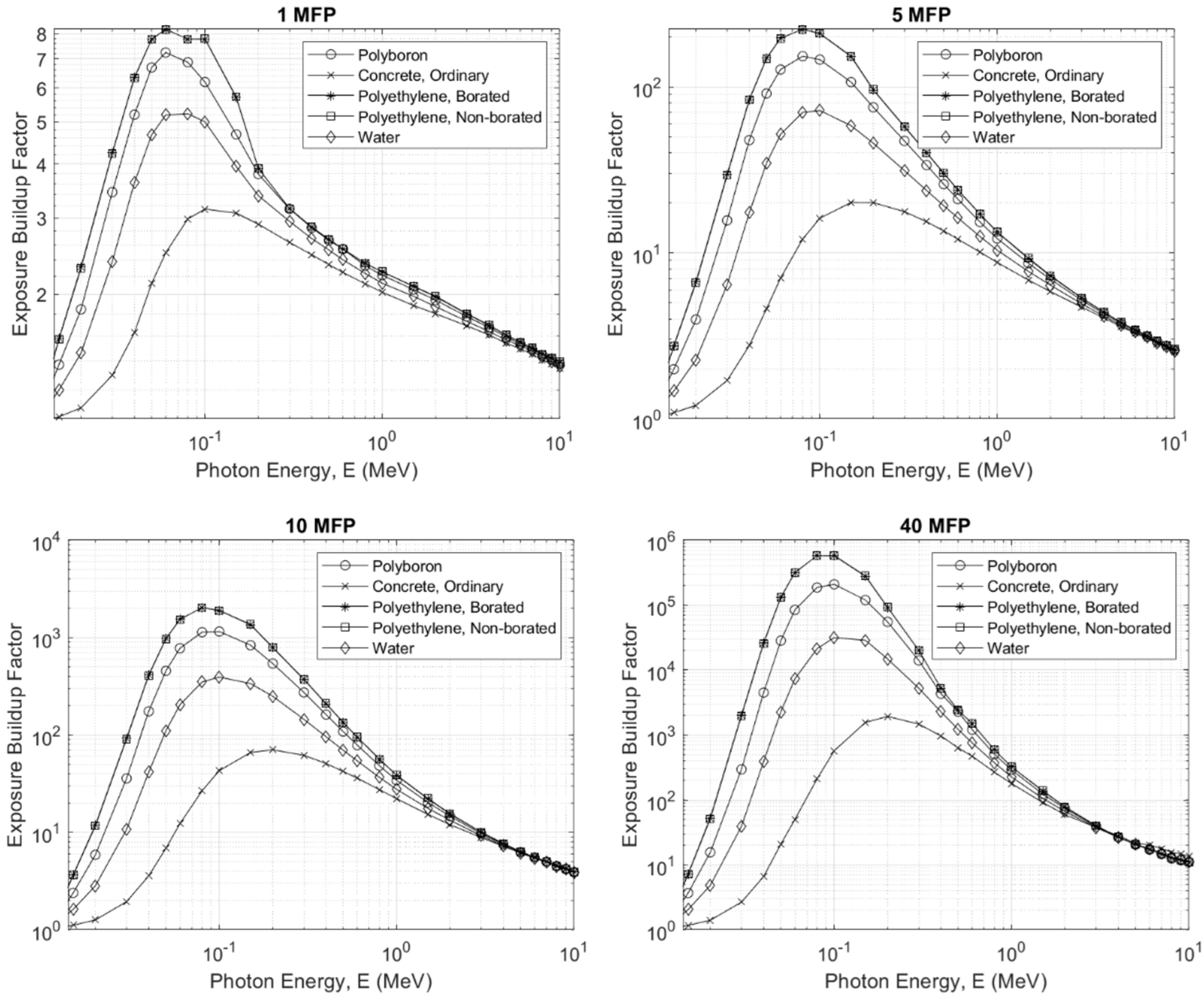

Figure 13: The EBF as a function of photon energy at 1, 5, 10, and 40 MFP depth.

MFP, polyboron EBF is moderate, higher than borated polyethylene and water but lower than concrete. At 5 MFP, polyboron EBF peak is higher, surpassing water and borated polyethylene, yet remaining below concrete. At 10 and 40 MFP, polyboron EBF becomes significantly pronounced, approaching the high values seen in ordinary concrete, indicating effective photon buildup at greater depths. Across all depths, polyboron demonstrates a consistent peak in EBF around 0.1 MeV, reflecting the dominance of Compton scattering in this energy range. The EBF values increase with depth, indicating substantial photon buildup at higher MFPs.

The variation in EBF with penetration depth at fixed incident photon energies of 0.015, 0.15, 1.5, and 3 MeV are shown in Fig. 14-a to 14-d. Polyboron exhibits higher EBF values at lower photon energies (0.015 and 0.15 MeV) compared to other shielding materials, indicating enhanced photon buildup and, consequently, more effective shielding at these energies. At higher photon energies (1.5 and 3 MeV), the differences in EBF among the materials decrease, leading to comparable shielding effectiveness.

The analysis of the EABF for polyboron, compared to ordinary concrete, borated polyethylene, non-borated polyethylene, and water, reveals trends similar to EBF. The variation in the EABF with photon energy at fixed penetration depths of 1, 5, 10, and 40 MFP are shown in Fig. 15-a to 13-d. Similarly, the variation in the EABF with penetration depth at fixed incident photon energies of 0.015, 0.15, 1.5 and 3 MeV is shown in Fig. 16-a to 13-d. Polyboron consistently shows effective energy absorption buildup, particularly at lower photon energies and deeper depths, outperforming borated polyethylene and water.

4.2 Neutron Attenuation Parameter

The fast neutron removal cross-section (Σ_R) is a critical parameter for assessing the effectiveness of materials in attenuating fast neutrons. This parameter indicates the probability of neutron interactions per unit length, which is essential for designing effective radiation shields in environments with significant neutron flux. A higher Σ_R value signifies better neutron attenuation capabilities, making the material more suitable for shielding applications. Σ_R calculations were performed using the Phy-X/PSD code, which utilized data adopted from Chilton et al. and Kaplan (Chilton et al., 1983; Kaplan, 1988). Additionally, the parameter was calculated from the fast neutron mass removal cross-sections reported by Hila et al. (Hila et al., 2023) and correlations proposed by Zollar

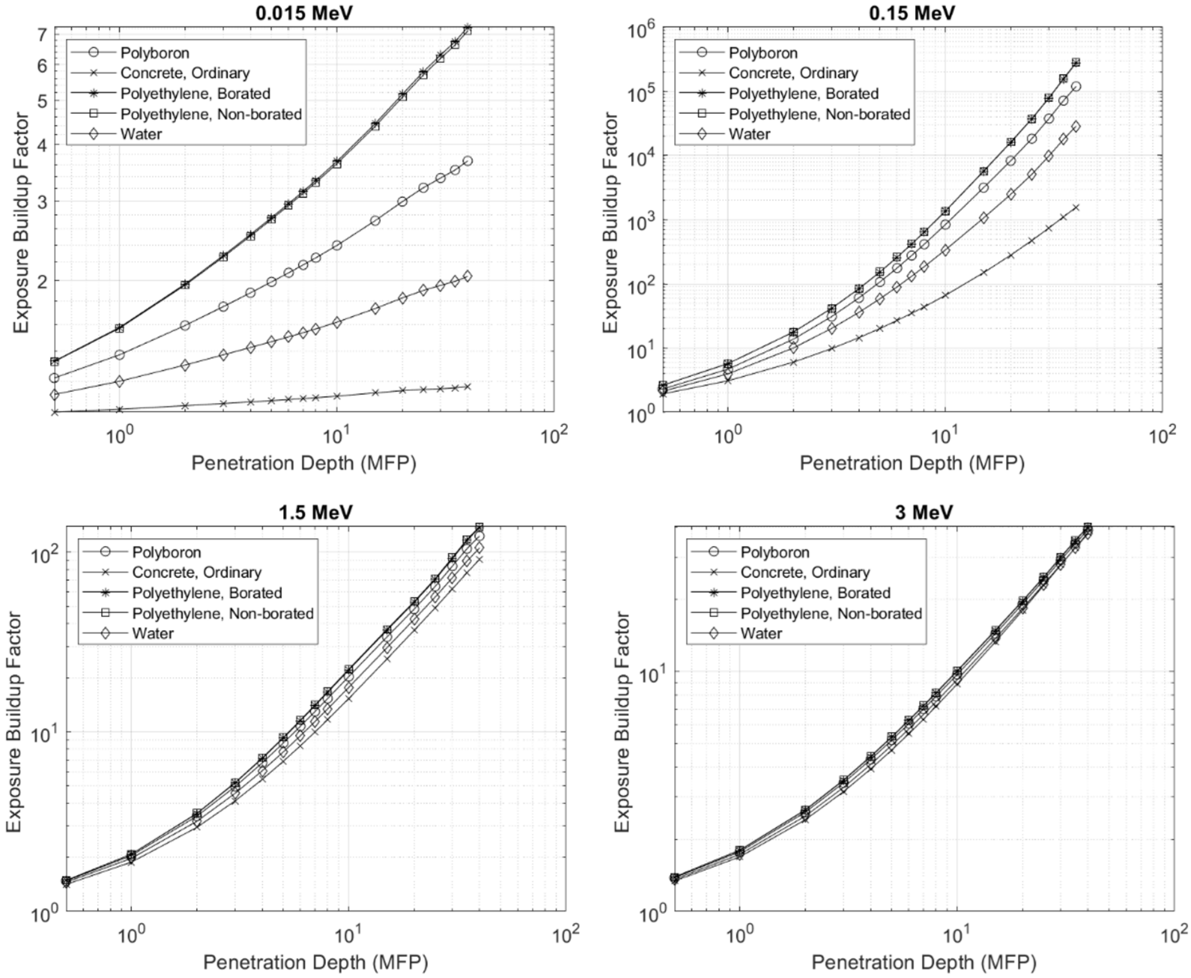

Figure 14: The EBF and penetration depth at photon energies 0.015, 0.15, 1.5, and 3 MeV.

Table 4: The Fast neutron removal cross-section (cm^2) for different shielding materials.

Material/ Method	Phy-X/PSD	Hila et al. (Hila et al., 2023)	Zollar (Zoller, 1964)
Polyboron	0.1128	0.1094	0.0637
Concrete, Ordinary	0.1108	0.1042	0.0889
Polyethylene, Borated	0.1196	0.1161	0.0684
Polyethylene, Non-borated	0.1199	0.1165	0.0654
Water	0.1027	0.0999	0.0572

(Zoller, 1964). Hila et al. generated the database using a variance-reduced sliced spherical shell Monte Carlo simulation model and the ENDF/B-VIII.0 neutron cross-section library. The data are given in Table 4, showing a comparison of results from different methods.

Polyboron has a fast neutron removal cross-section of 0.11279 cm^{-1} as calculated by Phy-X/PSD, which is slightly higher than ordinary concrete (0.11083 cm^{-1}) and water (0.10270 cm^{-1}). It is slightly lower than both borated polyethylene and non-borated polyethylene, each with a Σ_R of approximately 0.11960 cm^{-1} and 0.11991 cm^{-1}, respectively. Results from Hila et al. (Hila et al., 2023) show similar trends, with polyboron at 0.10941 cm^{-1}, again higher than concrete (0.10423 cm^{-1}) and water (0.09989 cm^{-1}) but lower than the polyethylenes. The values obtained from Zoller are lower overall, with polyboron at 0.06374 cm^{-1}, which still shows its effectiveness compared to concrete and water but less so than the polyethylenes. This indicates that polyboron is highly effective in neutron attenuation, outperforming conventional materials like concrete and water, and is only marginally less effective than polyethylenes.

It is important to emphasize the physical mechanism driving this performance. While heavy metals such as iron (Fe) exhibit excellent inelastic scattering cross-sections for highly energetic fast neutrons, they are remarkably inefficient at elastically scattering and thermalizing neutrons to lower energies (Chilton et al., 1983). Consequently, heavy metals cannot effectively eliminate neutron flux on their own and require the addition of a moderating medium. Polyboron circumvents this limitation through its high hydrogen content, derived from polyethylene and paraffin wax which rapidly thermalizes fast neutrons via elastic scattering, while its boron ester com-

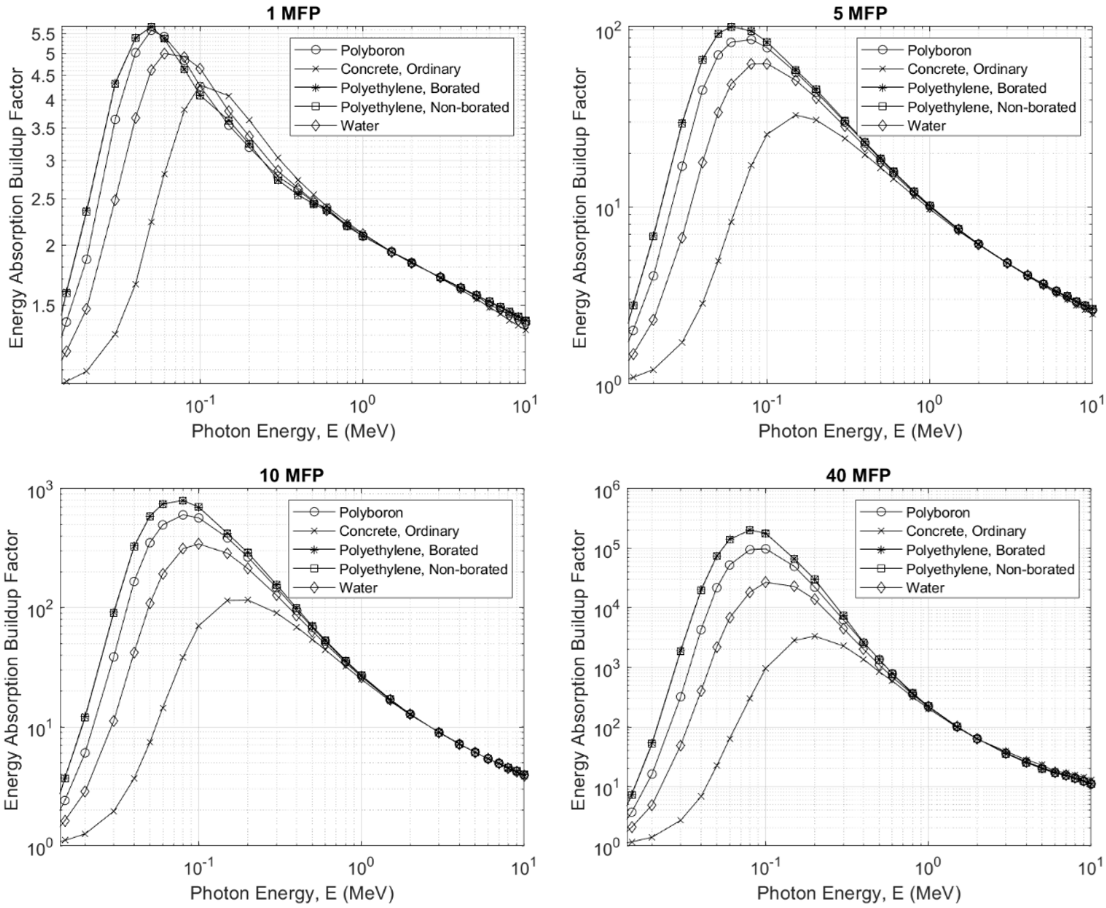

Figure 15: The EABF as a function of photon energy at 1, 5, 10, and 40 MFP depth.

ponent captures the resulting thermal neutrons without generating high-energy secondary capture gammas. By achieving this comprehensive, self-contained neutron attenuation at a fraction of the physical weight of metallic shields (~0.97 g.cm^{-3} compared to iron's ~7.87 g.cm^{-3}), Polyboron provides a distinct operational advantage for weight-restricted environments.

4.3 Validation of Computational Method

To ensure the reliability of the calculated shielding parameters, a two-tiered benchmarking method was employed. First, a rigorous code-to-code computational validation was performed. The results obtained from the MATXCOM program (based on the EPICS2023 library) were benchmarked point-by-point against the well-established Phy-X/PSD software (Islam, 2025; Şakar et al., 2020) over the continuous energy spectrum (1 keV to 20 MeV). The benchmarking metric evaluated the relative percentage deviation between the two codes. As shown in Fig. 1, the Mass Attenuation Coefficients (MAC) calculated by both methods show excellent agreement. For instance, at 1 MeV, the MAC values for polyboron are identical (0.071 cm^2.g^{-1}) for both MATXCOM and Phy-X/PSD, and the relative deviation across all energies remains consistently below 1%. This high degree of concordance confirms the accuracy of the algorithm and the proper implementation of the underlying nuclear data libraries used in this study.

Second, an empirical validation was conducted to connect the theoretical calculations to physical reality. The computed Linear Attenuation Coefficient (LAC) values and fast neutron removal capabilities were evaluated against experimental trends observed in the foundational work of Bhuiyan et al. and Ahmed et al. (Ahmed et al., 1992; Bhuiyan et al., 1989), who physically synthesized and tested polyboron slabs using a Cf-252 source. While direct point-to-point comparisons are constrained by the specific source emission spectra used in those early experiments, the energy-dependent attenuation behavior observed in our simulation strongly aligns with the physical measurements of the material's density and effective removal capability. This dual benchmarking method, combining quantitative computational cross-verification with qualitative consistency against historical experimental data demonstrates that the analytical model used in this work provides a physically accurate and reliable representation of polyboron's radiological properties.

5 Conclusions

This study demonstrates a critical engineering advancement for mixed-field radiation environments: Polyboron achieves a 1.8% improvement in fast neutron removal capability compared to ordinary concrete, yet it does so while providing a massive 57.8% reduction in structural

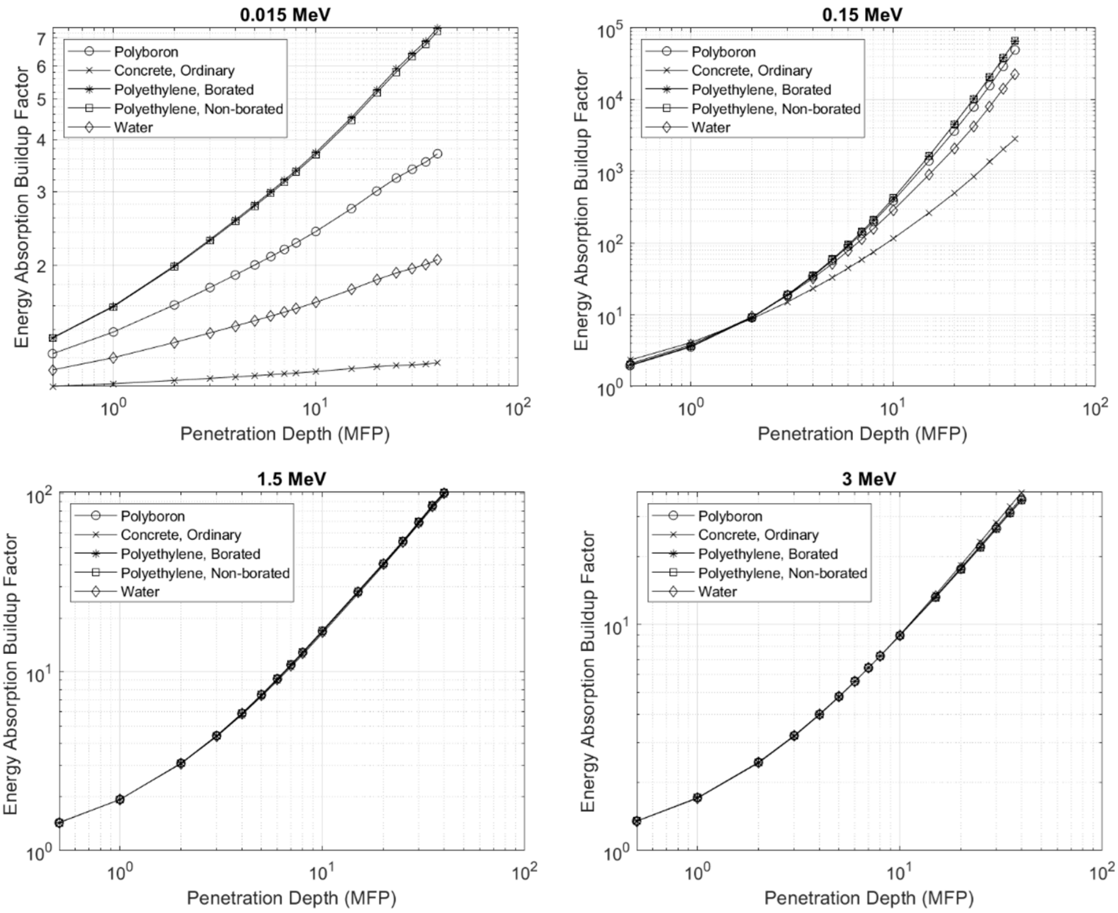

Figure 16: The EABF and penetration depth at photon energies 0.015, 0.15, 1.5, and 3 MeV.

weight. By providing the neutron protection of heavy concrete without the associated weight penalty, this material establishes a vital structural trade-off for nuclear applications. Furthermore, comprehensive analysis confirms its function as a highly efficient dual-purpose shield. Polyboron operates as a competent intermediate-Z photon shield, exhibiting an approximate 9.2% advantage in mass attenuation coefficient (MAC) over concrete at 1 MeV and predictable attenuation behavior at high penetration depths. Consequently, Polyboron is not merely a viable substitute, but a superior, high-performance alternative specifically engineered for weight-sensitive deployment. It is uniquely suited for mobile nuclear shielding, transport casks for medical isotopes, and research reactor beamlines, where minimizing structural load is as critical as maximizing radiological safety.

Conflict of Interest

The authors declare no potential conflict of interest regarding the publication of this work.

Funding

The authors declare that no funds, grants, or other financial support were received during the preparation of this manuscript.

References

Ahmed, F., Bhuiyan, S., Mollah, A., et al. (1992). Measurements of gamma-ray shielding properties of ilmenite-magnetite concrete and polyboron slabs using a Cf-252 source. *Nuclear technology*, 98(3):379–386.

Akman, F., Durak, R., Turhan, M. F., et al. (2015). Studies on effective atomic numbers, electron densities from mass attenuation coefficients near the K edge in some samarium compounds. *Applied Radiation and Isotopes*, 101:107–113.

Bhuiyan, S., Ahmed, F., Mollah, A., et al. (1989). Studies of the neutron transport and shielding properties of locally developed shielding material: poly-boron. *Health Physics;(USA)*, 57(5).

Biswas, R., Sahadath, H., Mollah, A. S., et al. (2016). Calculation of gamma-ray attenuation parameters for locally developed shielding material: Polyboron. *Journal of Radiation Research and Applied Sciences*, 9(1):26–34.

Chilton, A. B., Shultis, J. K., and Faw, R. E. (1983). Principles of radiation shielding.

Detwiler, R. S., McConn, R. J., Grimes, T. F., et al. (2021). Compendium of material composition data for radiation transport modeling. Technical report, Pacific Northwest National Laboratory (PNNL), Richland, WA (United States).

Han, I. and Demir, L. (2009a). Determination of mass attenuation coefficients, effective atomic and electron numbers for Cr, Fe and Ni alloys at different energies. *Nuclear Instruments and Methods in Physics Research Section B: Beam Interactions with Materials and Atoms*, 267(1):3–8.

Han, I. and Demir, L. (2009b). Studies on effective atomic numbers, electron densities from mass attenuation coefficients in TixCo1- x and CoxCu1- x alloys. *Nuclear Instruments and Methods in Physics Research Section B: Beam Interactions with Materials and Atoms*, 267(21-22):3505–3510.

Harima, Y. (1983). An approximation of gamma-ray buildup factors by modified geometrical progression. *Nuclear Science and Engineering*, 83(2):299–309.

Hila, F. C., Jecong, J. F. M., Dingle, C. A. M., et al. (2023). ENDF/B-VIII. 0-based fast neutron removal cross sections database in Z= 1 to 92 generated via multi-layered spherical geometry. *Radiation Physics and Chemistry*, 206:110770.

Islam, S. (2025). MATXCOMan x-ray/gamma-ray attenuation calculator for arbitrary materials based on EPICS2023 evaluated photon data library. *Radiation Physics and Chemistry*, 229:112433.

Kaplan, M. F. (1988). Concrete radiation shielding.

Manjunatha, H. (2017). A study of gamma attenuation parameters in poly methyl methacrylate and Kapton. *Radiation Physics and Chemistry*, 137:254–259.

Şakar, E., Özpolat, Ö. F., Alım, B., et al. (2020). Phy-X/PSD: development of a user friendly online software for calculation of parameters relevant to radiation shielding and dosimetry. *Radiation Physics and Chemistry*, 166:108496.

Trubey, D. K., Eisenhauer, C. M., Foderaro, A., et al. (1991). Gamma-ray attenuation coefficients and buildup factors for engineering materials.

Zoller, L. (1964). Fast-neutron-removal cross sections. *Nucleonics (US) Ceased publication*, 22.

To cite this article:

S. M. Nymul Hasan Anik, S. Islam, A. Mahdi (2026). EPICS2023-based evaluation of polyboron as a gamma-ray and fast-neutron shielding material. *Radiation Physics and Engineering*, In Press.

DOI:

To link to this article: